

Oscillatory magnetic properties

by R. Allenspach
W. Weber

The recent discovery of oscillations in interlayer exchange coupling as a function of nonmagnetic spacer layer thickness has led to a widespread interest in oscillatory magnetic properties in layered structures for both basic and applied reasons. In this overview, several oscillatory magnetic properties are discussed for a particular model system. We have chosen epitaxial fcc Co films grown on Cu(100) as a base structure and have selected additional epitaxial overlayers to study interlayer exchange coupling, induced magnetic moments, magneto-optical properties, and magnetic anisotropy.

1. Introduction

The discovery that the exchange coupling between two ferromagnetic layers separated by a nonmagnetic spacer material oscillates with varying spacer thickness [1–3] has prompted a wealth of investigations, revealing that other magnetic properties such as giant magnetoresistance [3–5], magneto-optical response [6–9], and magnetic anisotropy [10, 11] also exhibit oscillatory behavior as a function of film thickness. Apart from morphology-induced oscillations, the occurrence of quantum size effects in the layered systems is believed to be the origin of the oscillations. The resulting quantum well (QW) states are electronic states confined within ultrathin films by the potential barriers at the surface or at the interface to the adjacent layers, giving rise to sharp structures in the electronic density of states. Experimentally, these QW states have indeed been observed in various systems [12–15].

In this paper selected oscillatory magnetic properties are discussed for a particular model system, starting with Co films epitaxially grown on Cu(100). For this system we have investigated the evolution of magnetic anisotropy with increasing film thickness and its relation to film morphology. Growing a Cu overlayer allows us to study the influence of a nonmagnetic film on the anisotropy and on the magneto-optical response. The Cu/Co/Cu(100) structure then serves as the basic building block for a systematic investigation of oscillatory exchange across a Cu spacer. We have added another ferromagnetic transition metal M and compare structures of the type $M/\text{Cu}/\text{Co}/\text{Cu}(100)$ with $M = \text{Fe}, \text{Co}, \text{or Ni}$. Alternatively, a paramagnet with a very large susceptibility has also been used to probe exchange oscillations directly within the paramagnet.

Section 2 discusses the comparative investigation of the exchange oscillations across the Cu spacer in some detail. The observation of oscillations in the magnetic anisotropy and the magneto-optical response are reported in Section 3. Concluding remarks are presented in Section 4.

2. Oscillatory exchange coupling

Long-range magnetic exchange coupling between transition metals was first discovered in Fe/Cr/Fe(001) [16], which exhibited an antiferromagnetic coupling of the Fe films across the Cr spacer layers. Subsequent studies have revealed the oscillatory behavior of the exchange coupling in this system [3] and its general occurrence in a wide variety of systems [17]. Various models have been proposed to account for the long range of this exchange coupling and to explain the oscillatory behavior that results in a periodic sequence of ferromagnetic (FM) and antiferromagnetic (AF) alignment of the adjacent

©Copyright 1998 by International Business Machines Corporation. Copying in printed form for private use is permitted without payment of royalty provided that (1) each reproduction is done without alteration and (2) the *Journal* reference and IBM copyright notice are included on the first page. The title and abstract, but no other portions, of this paper may be copied or distributed royalty free without further permission by computer-based and other information-service systems. Permission to *republish* any other portion of this paper must be obtained from the Editor.

magnetic layers. Theoretical approaches based on quantum confinement [18, 19] and on the Ruderman-Kittel-Kasuya-Yosida (RKKY) interaction [20, 21] have been able to describe the origin of the coupling. As predicted by the RKKY model, experiments have shown that the periods depend on the spacer material and its crystallographic orientation [22]. Recently, it has been found that the oscillations also occur with the magnetic layer thickness [23] or even with the thickness of a nonmagnetic overlayer [24]. These results can be understood in terms of a QW model. Indeed, oscillations with varying magnetic film thickness have been predicted to be caused by a confinement within the ferromagnet [25]. Amplitudes and phases of the oscillations, however, are more complicated to understand because they are influenced by each layer in an entire multilayer stack, as has recently been predicted [26].

• *Coupling across Cu(100)*

One particular spacer material has stimulated considerable interest: Cu(100). Exchange coupling across a noble metal is relatively easy to model using an RKKY perturbation theory. Moreover, since the Fermi surface of the (100) surface has two different stationary spanning vectors, the exchange coupling J is a superposition of two sine waves, varying with increasing Cu thickness d as $J(d) = 1/d^2[A_1 \sin(2\pi d/\Lambda_1 + \phi_1) + A_2 \sin(2\pi d/\Lambda_2 + \phi_2)]$. Within the RKKY model, the short and long periods are predicted to be $\Lambda_1 = 2.56$ monolayers (ML, 1 ML = 0.18 nm) and $\Lambda_2 = 5.88$ ML, with the corresponding ratio of amplitudes $A_1/A_2 = 3.7$ [21]. Although the same periods are found within the QW model, the amplitude ratio there is much larger, $A_1/A_2 = 9-320$ [27-29], so there should be practically no contribution of the long period. This difference exists because the RKKY model—in contrast to the QW model—does not contain all of the factors that determine the amplitude ratio. The first factor, which is included in RKKY theory, is the topology of the Cu Fermi surface. A second factor is the degree of confinement within the Cu spacer layer. It is determined by matching the electronic bands at the interface, and is not included in RKKY theory.

Therefore, the agreement of the periods and the disagreement of the amplitudes are related to the fact that the calculation of the periods is more reliable because periods are determined exclusively by the spacer material. The amplitudes and phases, however, are also influenced by the band matching at the interface and hence by the FM material.

Cu(100) is also exceptional from an experimental point of view. Its crystal structure and lattice constant are such that the three transition-metal ferromagnets Fe(100), Co(100), and Ni(100) grow epitaxially onto it. This enables us to compare oscillatory exchange coupling through

Cu(100) using various FM layers—in order to determine not only periods but also amplitude ratios and peak shifts, i.e., phases. Shifts of the most prominent AF peak have been investigated on sputtered multilayers [30]. Recently, this work was extended to epitaxial Co, Ni, and Ni alloys in symmetric structures of the type $M/\text{Cu}/M(100)$ [31].

We have chosen a different approach to minimize the effects of roughness and interdiffusion at the interface, which can lead to systematic offsets in the Cu thickness and hence in the phases. *Asymmetric* structures of the type $M/\text{Cu}/\text{Co}(100)$ are grown onto a Cu(100) single-crystal substrate, where $M = \text{fcc Fe, fcc Co, or fcc Ni}$. This maintains an *identical* interface between the Co base layer and the Cu spacer as well as *identical* growth of the Cu spacer. The only difference arises from the second interface and the top FM film.

We observe the oscillations in exchange coupling by spin-polarized scanning electron microscopy (spin-SEM) [32-34]. The signal obtained is the spin polarization P of the secondary electrons originating in approximately the top five surface layers. The capability of this technique to detect the exchange oscillations has been established in experiments on Fe/Cr/Fe [33]. By recording P of the top FM layer, spin-SEM provides a direct map of the sign of the exchange coupling on wedge-type samples. This allows very weak AF coupling to be distinguished from FM coupling, which is not possible with the more commonly employed technique of recording the switching field in magnetic hysteresis loops. On the other hand, a direct determination of the exchange amplitude is not possible.

In order to compare various FM top layers, we grow wedge structures of the type shown in **Figure 1** by molecular beam epitaxy. To eliminate offsets between the various top layers of the same structure, the lateral distance between Co and Fe or Ni is kept below 100 μm . The onset of the wedge is seen directly in the SEM to within 0.1 ML because the yield of secondary electrons differs for different materials [35]. The absolute thickness of the Cu spacer is correct to within 5%, calibrated using scanning Auger microscopy and cross-checked with a stylus profilometer.

The thickness of the bottom Co layer is 10 to 15 ML; that of the top Co or Ni layer is between 8 and 15 ML. At this thickness the exchange oscillations within the ferromagnet itself are expected to be suppressed [19, 23]. The thickness of the Fe top layer is restricted to 2.7-3.9 ML, because fcc Fe is paramagnetic outside this thickness range at our measuring temperature of 300 K (see the section on direct probing of the oscillatory exchange coupling within a paramagnet and Reference [36]).

Co/Cu/Co(100)

Several experiments have established the existence of two coupling periods, $\Lambda_1 \approx 2.6$ ML and $\Lambda_2 \approx 5.5-8.0$ ML

[22, 37, 38], and a ratio of amplitudes of $A_1/A_2 = 1.25$ [39]. Although the agreement with theory is satisfactory for the periods, the predicted amplitude ratio is off by at least one order of magnitude compared to the most recent calculations [19, 28, 29]. We have found that this discrepancy originates in the specific sample investigated and is not of fundamental origin (see Figure 2). Long-period oscillations with only a few short-period oscillations are visible for the wedge structure (a), whereas the behavior for structure (b) displays an array of short-period oscillations.

We determine periods and amplitude ratios directly from a Fourier transform, and subsequently check the results using the methods described in Reference [40]. Although this technique measures the sign of the coupling rather than the strength, the analysis works very reliably because of the large number of sign reversals up to a high spacer thickness. This holds for both periods and amplitude ratios. We emphasize, on the other hand, that no conclusions concerning the absolute amplitudes can be drawn with this approach. Sample (a) yields $\Lambda_1 = 2.73$ ML and $\Lambda_2 = 6.00$ ML. From sample (b) we obtain only the short period $\Lambda_1 = 2.58$ ML. The statistical uncertainty of the periods is 3%. The periods agree very well with calculations [19, 21, 28].

The amplitude ratio varies strongly when going from sample (a) to (b): $A_1/A_2 = 0.6 \pm 0.3$ for (a) and >7 for (b). We note that the substrates used were two different Cu single crystals. Scanning tunneling microscopy (STM) on the substrates indicated that both substrates exhibited a stepped surface with atomically flat terraces having a length exceeding 300 nm and an average width of 6.5 nm [sample (a)] and 3.5 nm [sample (b)]. It is unclear how these differences in the substrate influence the growth mode of the spacer. On the basis of previous studies [33], we attribute the difference of the amplitude ratio in our samples to the roughness of the films: The short-period oscillations become more pronounced if the roughness of the spacer is reduced [33]. We conclude that the much-debated discrepancy between the large predicted amplitude ratio [19, 28, 29] and the much smaller experimental value [39] is absent in sample (b), where $A_1 \gg A_2$. Moreover, our experiment clearly shows that a proper description of the exchange coupling has to go beyond RKKY theory, which is unable to explain such a large amplitude ratio.

M/Cu/Co(100) ($M = fcc$ Fe, Ni)

In order to investigate the influence of ferromagnetic material on exchange coupling, we turn to asymmetric structures, *M/Cu/Co(100)*, where $M = \text{Fe}$ or Ni . On the same Cu wedge, we grow next to the Co layer either an Fe or a Ni layer. Line scans from the spin-SEM images obtained with increasing Cu thickness are shown in

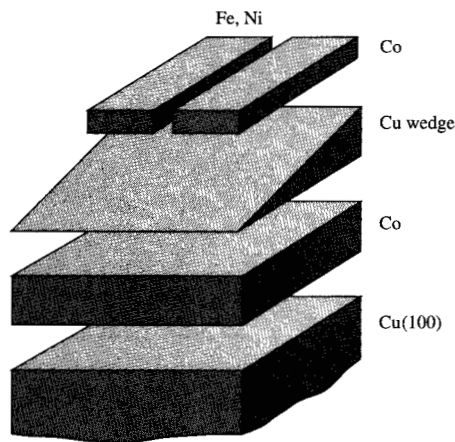


Figure 1

Stacking of the magnetic structures used in the investigation of exchange coupling across Cu(100). The layers shown were grown by molecular beam epitaxy.

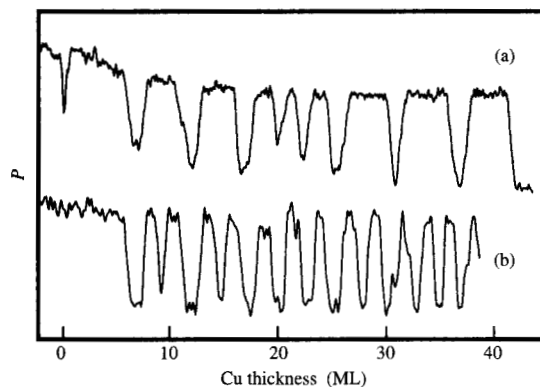


Figure 2

Spin polarization P (or sign of exchange coupling) vs. Cu spacer thickness (in monolayers) for two Co/Cu/Co(100) samples [(a) and (b)]. More gradual transitions between FM and AF are observed because the line scans average over a sample region of $\approx 50 \mu\text{m}$. The peak near 0 ML in (a) is caused by an anisotropy-induced change of the magnetization direction (see the subsection on magnetic anisotropy). Data to the left of 0 ML correspond to the scan portion before the wedge starts.

Figure 3. We deduce the following results: 1) The long oscillation period is independent of the choice of FM film, confirming that the period is determined exclusively by the spacer material. 2) The phase of the long-period

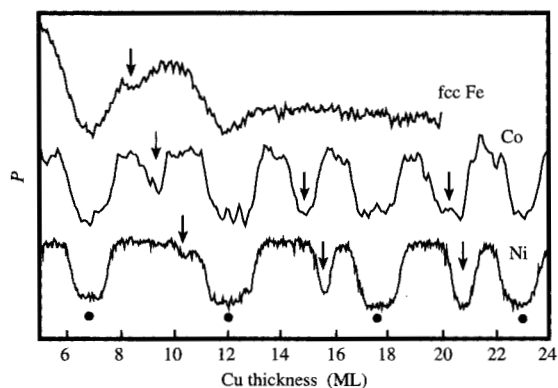


Figure 3

Spin polarization P vs. Cu spacer thickness for an $M/\text{Cu}/\text{Co}(100)$ structure with Fe, Co, and Ni as the upper film M . The positions of the first four AF peaks derived from long-period oscillations are indicated by dots. Note the peak shifts of the short-period oscillations (arrows). From [50], reproduced with permission.

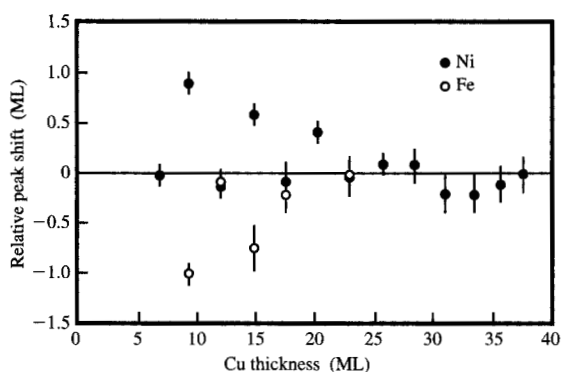


Figure 4

AF peak positions vs. Cu spacer thickness in $M/\text{Cu}/\text{Co}(100)$ structures relative to the position of the $\text{Co}/\text{Cu}/\text{Co}(100)$ reference structure, with $M = \text{Fe}$ (open circles) and Ni (solid circles).

oscillation is identical in all films. 3) The short-period AF peaks in Ni and Fe are shifted in comparison to Co, and their relative positions also vary with increasing Cu thickness.

The primary and new result of Figure 3 is the different behavior of long- and short-period oscillations in Ni compared to Co. Whereas the AF peak positions for the long-period oscillations coincide, the short-period AF peaks do not. From a Fourier transform we deduce $A_1/A_2 = 1.3 \pm 0.5$ for Ni, compared to $A_1/A_2 = 3.5 \pm 1.0$

for Co on this particular wedge: The amplitude ratio is found to decrease on going from Co to Ni.

It is surprising that only some of the peaks shift. As $\Lambda_2 \approx 2\Lambda_1$, short-period derived peaks are superimposed on most of the long-period AF peaks. Thus, the shift of the short-period peaks should also result in a shift of peaks such that both short- and long-period peaks are present. That we do not observe such shifts is a clear indication that the coupling strength of the short-period oscillations is weakened in comparison to the long-period oscillations at thinner Cu spacer thickness. As a result only the peaks of exclusively short-periodic origin (marked by arrows in Figure 3) shift, whereas those having contributions from both long- and short-period oscillations (marked by dots) do not. Thus, the amplitude ratio given above has to be interpreted as an average over the entire Cu thickness range investigated.

It is more difficult to observe short-period oscillations in fcc Fe/Cu/Co(100) structures because Fe/Cu(100) is intrinsically perpendicularly magnetized [34]. One of the few films that exhibit indications of short-period oscillations is shown in Figure 3. Again, a shift is observed for this peak, $-0.37\Lambda_1$, but not for the long-period oscillations. This finding is at variance with Reference [19], which calculates a shift for both long- and short-period oscillations.

The short-period peak shifts compared to the Co/Cu/Co(100) system for both Ni and Fe are compiled in Figure 4. For the first short-period peak, fair agreement with other experiments [31] is found. In particular, the signs of the shifts agree. The peak shift is positive for Ni and negative for Fe. This behavior can be understood in terms of an extension of the Friedel-Anderson-Caroli model [41], which relates peak shifts basically to band filling. As the Co band is less (more) filled than the Ni (Fe) band, a positive (negative) peak shift is predicted for Ni (Fe) compared to Co. However, no difference between long- and short-period oscillations is expected in this simple model, contrary to our observation. We ascribe this discrepancy to the different confinement of the electronic states being responsible for long- and short-period oscillations. It has been shown that the states leading to the long-period oscillations are only weakly confined, whereas the ones leading to the short-period oscillations are almost completely confined [28]. Reflection at the potential well should thus lead to a strong phase shift for the short-period oscillations and a much smaller one for the long-period oscillations.

However, the agreement of the phases of long-period oscillations for all three ferromagnetic fcc metals is still surprising, because interdiffusion is likely to occur and may be different for the three metals. In the case of fcc Fe on Cu(100), for instance, significant interdiffusion has been observed [42]. A coincidental cancellation of

interdiffusion-induced and intrinsic phase shift is very unlikely to occur. Thus, the agreement of the phases suggests that an amount of interdiffusion similar to that in the Fe/Cu system should also be found for Co/Cu and Ni/Cu. In fact, interdiffusion comparable to that reported for Fe/Cu(100) has recently been observed for Co/Cu(100) [43].

With increasing Cu thickness, the peak shifts of the short-period oscillations in Figure 4 decrease and eventually vanish. We note that the data of Figure 4 do not depend on assumptions or fitting procedures: They are given directly by the peak position differences of the spin-SEM line scans. Thus, we cannot deduce a well-defined phase shift from the peak shifts observed, because a phase shift is by definition a constant quantity for all spacer thicknesses. An immediate conclusion from this result is that it is very risky to deduce phase shifts from only the first or second AF maximum, as has been done in the past [31]. There is still no explanation for this peculiar behavior of the peak shifts. We presume that the pre-asymptotic RKKY regime might extend to much larger thicknesses than previously anticipated.

- *Direct probing of the oscillatory exchange coupling within a paramagnet*

In the preceding section we have seen that the exchange coupling across a spacer layer manifests itself as a periodic sequence of FM and AF alignment of the FM layers. These oscillations are explained by the RKKY model [20, 21], which assumes an oscillation of the spin density within the spacer material. In principle, only one interface to a ferromagnet should be sufficient to provoke such a spin polarization in the spacer, at least to some extent. Thus, we expect to see also an oscillatory magnetic moment within the spacer layer by probing the electrons emerging from the spacer material. However, standard spacer materials, such as the noble metals Au or Cu, have low magnetic susceptibilities; hence, the induced magnetic moments should be extremely small. In fact, recent experiments have shown that even the induced magnetic moment right at the interface, where the strongest effects due to hybridization are expected, is as small as $0.05 \mu_B$ in noble metals [44].

In order to probe the exchange oscillations directly in the spacer material, the magnetic signal arising from the nonmagnetic spacer must be increased. A straightforward idea would be to use a spacer material having a high susceptibility, such as a ferromagnet above the Curie temperature T_C , because in ultrathin films the susceptibility above T_C is strongly enhanced [45]. We note that this high susceptibility is caused by d electrons rather than s, p electrons, which have an induced magnetic moment that is too small to be detected. Very recently, this approach has been carried out with paramagnetic fcc

Fe on Co(100) [46]. However, an oscillatory magnetic moment within the paramagnetic Fe has not been observed. We have chosen a slightly different approach. Instead of having the fcc Fe in direct contact with the Co underlayer, we separated them with a standard spacer. The greater magnetic contrast in the high-susceptibility paramagnet then directly reflects the oscillations of the exchange coupling field at the surface of the low-susceptibility spacer material. Moreover, upon increasing the thickness of the paramagnetic overlayer, oscillatory behavior of the induced magnetization in the paramagnet is observed.

We have realized such a structure by growing a 7-ML Co film onto a Cu(100) substrate as the FM layer. After adding a Cu spacer layer, we deposit fcc Fe at room temperature. Except for a small thickness interval, $2.7 < d_{Fe} < 3.9$ ML, the Curie temperature T_C of fcc Fe on Cu(100) is below room temperature [36]. It is therefore an ideal system to investigate the influence of the exchange coupling field in a paramagnet with large susceptibility.

Magnetic data are obtained with three complementary experimental techniques performed in two different ultrahigh-vacuum chambers. For a spatially resolved characterization on double-wedge samples, we have used spin-SEM. Two additional techniques complement spin-SEM with respect to the probing depth: Spin-polarized low-energy electron diffraction (SPLEED) [47] has a very high surface sensitivity (≈ 2 ML) and the magneto-optical Kerr effect probes ≈ 50 ML [48]. As no lateral resolution is available in our setup for these additional techniques, no wedge samples have been investigated. Instead, the thickness dependence of magnetization in fcc Fe at fixed Cu thickness is measured by recording the SPLEED exchange asymmetry A_{ex} and the Kerr signal $I(H = 0)$ during deposition. Both quantities probe the strength of the remanent magnetization along the chosen in-plane direction. In this way a broad range of probing depths can be covered.

Paramagnetic fcc Fe as spacer

We first discuss the double-wedge structures grown for the spin-SEM experiments, consisting of a 7-ML Co/Cu(100) base structure, a Cu wedge, and an Fe wedge rotated by 90° with respect to the Cu wedge. From these experiments we can establish that the paramagnetic fcc Fe probes the sign of the exchange oscillations at the Cu wedge surface and that it acts as an additional spacer material. **Figure 5** shows line scans along the Cu wedge without Fe coverage (a) and for Fe overlayer thicknesses of (b) 1.6 ML and (c) 5.7 ML. Without Fe coverage, a pure exponential decay of the spin polarization P of Co with increasing Cu thickness is found. In particular, no oscillatory behavior is observed, in contrast to the Au/Fe(110) system [49]. The line scan for $d_{Fe} = 1.6$ ML, on the other hand, clearly shows

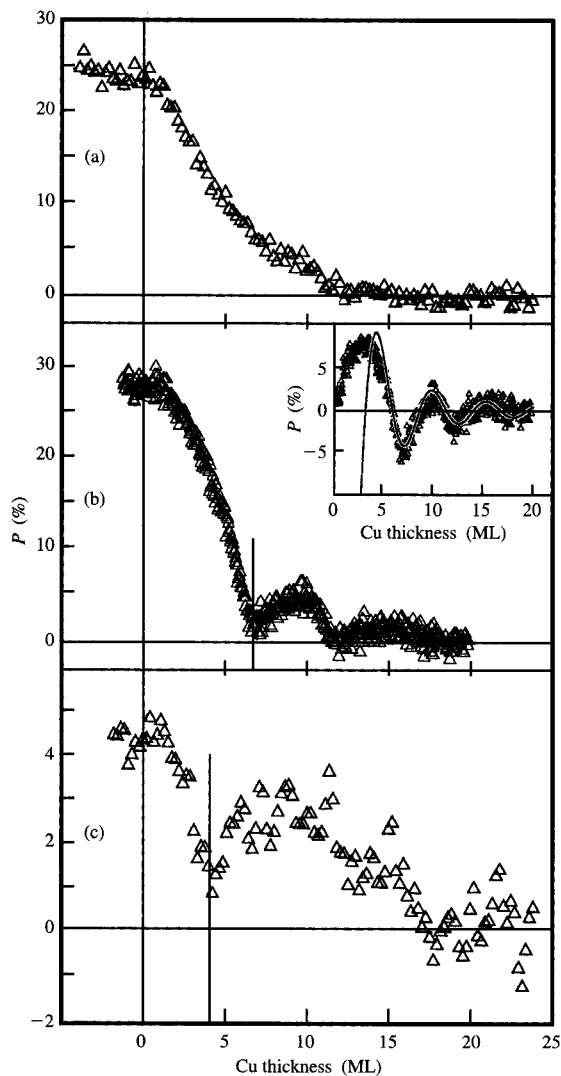


Figure 5

Line scans across double-wedge structures of fcc Fe/Cu/Co/Cu(100) obtained using spin-SEM. Spin polarization P vs. Cu spacer thickness is shown for three Fe overlayer thicknesses: (a) $d_{\text{Fe}} = 0$ ML, (b) $d_{\text{Fe}} = 1.6$ ML, and (c) $d_{\text{Fe}} = 5.7$ ML. The first AF peaks in (b) and (c) are marked by lines for comparison. The inset in (b) shows oscillatory behavior after subtraction of an exponential background and the theoretical fit curve described in the text. The different starting values of spin polarization at vanishing Cu thickness are caused by the different Fe coverages on top of the Co(100). From [36], reproduced with permission.

oscillations. After subtracting an exponential background, we compare the remaining oscillations with the oscillatory exchange field originating from the Co layer: $H_{\text{ex}} \propto 1/d^2 \sin(2\pi d/\lambda + \phi)$, where d is the spacer thickness, λ the

oscillation period, and ϕ the phase. The best agreement is reached for $\lambda = 5.6$ ML, which is close to the long period of the exchange coupling across Cu(100) [22, 50]. The fit confirms the $1/d^2$ dependence, a behavior that is expected of a paramagnet under the influence of an oscillatory exchange coupling field.

More insight can be gained from the line scan at $d_{\text{Fe}} = 5.7$ ML [see Figure 4(c)]. Again the first AF peak is visible, albeit with a peak shift of about 3 ML compared to the corresponding extremum for $d_{\text{Fe}} = 1.6$ ML, whereas the second AF peak cannot be identified. The peak shift between the different Fe thicknesses indicates that parts of the paramagnetic Fe film behave like an additional spacer. This finding is corroborated by a recent experiment involving Co/fcc Fe/Co(001) [46], where AF coupling across the paramagnetic Fe spacer layer with a period of 6 ML has been observed.

Induced magnetization oscillations within paramagnetic fcc Fe

The above results show that our approach is valid: If a paramagnet has a very large susceptibility, the exchange oscillations can be probed directly within the paramagnet. In this section we show that the amplitude of these oscillations is large enough that even a sign change of the oscillations within the paramagnet is observable. We reach this conclusion by comparing spin-SEM, SPLEED, and magneto-optical Kerr data to monitor a magnetic depth profile within the paramagnetic fcc Fe. **Figure 6** shows a spin-SEM line scan at $d_{\text{Cu}} = 3$ ML, as well as SPLEED and Kerr data for the same Cu thickness. The immediate increase of A_{ex} in Figure 6(a) to sizable values upon Fe deposition confirms that submonolayer Fe films are polarized in-plane by the exchange field arising from the underlying Co layer. The value of A_{ex} increases with Fe coverage of up to 2.7 ML, where T_{C} is still below room temperature. Upon further Fe deposition, T_{C} increases above room temperature. For Fe thicknesses above 3.9 ML, where T_{C} is again below room temperature, a drop to negative values is observed, indicating that the magnetization within the top Fe layers has changed sign. Upon further deposition, A_{ex} changes sign again before it ultimately vanishes. The oscillation period within the Fe overlayer extracted from the first AF and the second FM peak is ≈ 6 ML. The agreement with the long oscillation period observed for Cu(100) spacers [22, 50] may be coincidental in view of the different Fermi surfaces of the two materials.

The spin polarization P in the spin-SEM experiment in Figure 6(b) follows the same oscillatory behavior, with the exceptions that the negative peak is not as pronounced and that no further sign change is detected at higher Fe coverages. This is in accordance with the fact that SPLEED is more surface-sensitive and thus is able to sort

out the differently magnetized top magnetic layers more effectively. The model of induced magnetization oscillations within the paramagnet is supported by detecting the overall magnetic signal of the structure by the Kerr effect [see Figure 6(c)]. The starting point is the Kerr intensity arising from the underlying Co film. With increasing Fe film thickness, a linear increase of the remanent signal $I(H = 0)$ whose maximum is at 3.9 ML is detected again. Interestingly, no change of slope is observed as the thickness enters the FM region (see the shaded region in Figure 6). This shows that the exchange coupling field for $d_{\text{Cu}} = 3$ ML, which corresponds to the first ferromagnetic maximum, is strong enough to fully saturate the paramagnetic Fe films for thicknesses up to 2.7 ML. An estimate based on the surface anisotropy in Fe/Cu(100) and the magnetization reorientation yields a field value of the order of ≈ 2 T [36]. The remanence decreases thereafter and reaches a minimum at a thickness of Fe for which A_{ex} and P are negative. The magnetization value of the minimum is 10% less than at $d_{\text{Fe}} = 0$. Taking into account the large probing depth of the Kerr effect of ≈ 50 ML, the pure Co signal at $d_{\text{Fe}} = 5.7$ ML is expected to be reduced by 10%. Thus, the net magnetization probed at $d_{\text{Fe}} = 5.7$ ML corresponds to that of Co only. This means that the total Fe magnetization, which consists of a negative value from the surface layers and the value of the underlying layers, vanishes. We conclude that the film underneath the surface must be polarized with a positive magnetization by the exchange field in order to cancel the negative surface contribution. Finally, further deposition of Fe causes a slight increase of the Kerr intensity, which can be ascribed to the change of the surface magnetization back to positive values.

These experiments prove that it is possible to observe directly the oscillations of the spin density existing in a paramagnetic spacer material. Our approach has been successful because we selected a spacer with an extremely high susceptibility, thus increasing the polarization of the d electrons to a detectable level.

3. Oscillatory magnetic anisotropy and magneto-optical response

• Determining magnetic anisotropies from hysteresis loops

There exist various well-established methods to determine magnetic anisotropies, such as torque experiments [51] and ferromagnetic resonance or Brillouin light-scattering techniques [52]. All of these techniques determine anisotropies accurately and reliably in a straightforward manner applicable to almost any thin-film system.

For our purpose—to determine changes in the magnetic anisotropies during film growth—these techniques are not well suited because they are too slow. Therefore we analyze the magnetic hysteresis loops determined from the

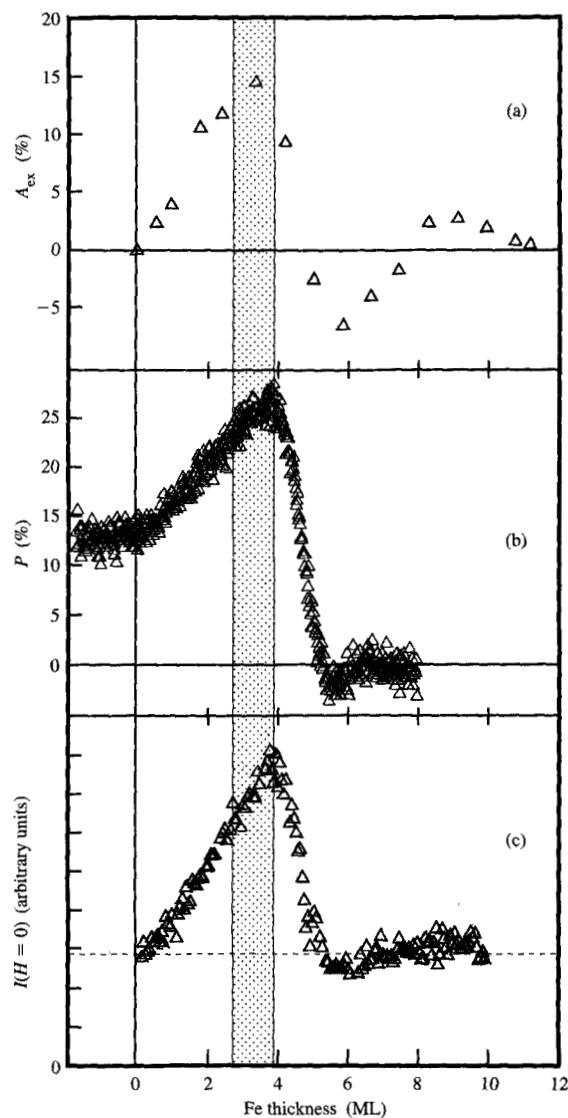


Figure 6

(a) Exchange asymmetry A_{ex} , (b) spin polarization P , and (c) remanent Kerr intensity $I(H = 0)$ as a function of Fe overlayer thickness d_{Fe} at a fixed Cu spacer thickness of 3 ML. The $I(H = 0)$ value of the dashed line in (c) corresponds to the starting value of the Kerr intensity at $d_{\text{Fe}} = 0$. The shaded part marks the thickness interval in which T_{C} of the Fe film is above room temperature, $2.7 \text{ ML} < d_{\text{Fe}} < 3.9 \text{ ML}$, as determined from the perpendicular magnetization component of spin-SEM images. Adapted from [36] with permission.

magneto-optical Kerr effect. This approach is fast and requires modest experimental efforts. Determining anisotropies from hysteresis loops, however, is usually very inaccurate or is based on assumptions concerning the

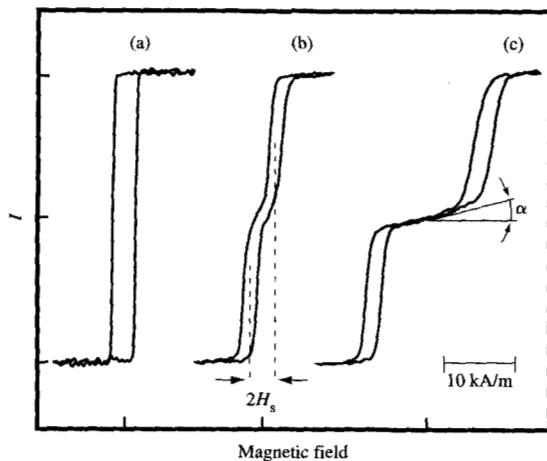


Figure 7

Hysteresis loops $I(H)$ obtained using the magneto-optical Kerr effect on a 2.5-ML Co film, grown on a stepped Cu substrate miscut by 0.1° with respect to the (100) orientation: (a) H along the $[1\bar{1}0]$ direction, (b) H along the $[110]$ direction, (c) same as (b) but having a bias field of $H_{\text{bias}} = 5 \text{ kA/m}$ along the $[1\bar{1}0]$ direction. The definition of the shift field H_s and of the linear initial slope s , with $s = \tan \alpha$, is indicated in (b) and (c).

magnetization-reversal mechanism. We show in the following that these limitations do not exist in a system with a superposition of twofold and fourfold anisotropies. Co films grown on a Cu(100) substrate with a well-defined preferential step arrangement exactly represent this class of systems.

The Cu(100) single-crystal substrate used in this study had a preferential step edge direction along $[1\bar{1}0]$, with an average step width of 100 nm. This leads to a slight miscut of 0.1° from the (100) orientation. Magnetic hysteresis loops were recorded *in situ* during the growth of the films using the magneto-optical Kerr effect, with the sample kept at a temperature of $\approx 320 \text{ K}$. **Figure 7** shows the hysteresis loops obtained from a Co film having a thickness of 2.5 ML, the magnetic field being applied either parallel (along $[1\bar{1}0]$) or perpendicular (along $[110]$) to the step edges of the Cu substrate. The easy magnetization axis runs parallel to the step edges, as shown by the rectangular hysteresis loop shape. The loop taken perpendicular to the step edges is more complicated. It comprises two single loops shifted against each other. This difference of the magnetic response in the $[1\bar{1}0]$ and the $[110]$ directions, which are magnetically equivalent on a perfect fourfold Co(100) film, is attributed to the steps and phenomenologically described by a uniaxial anisotropy energy [53–55]. Whereas the $[1\bar{1}0]$

direction is the easy magnetization axis, the $[110]$ direction is the intermediate axis because it combines the easy character of the fourfold cubic anisotropy with the hard character of the uniaxial anisotropy. For composite hysteresis loops along the intermediate axis, we define a shift field H_s as the field difference between zero field and the center of one of the shifted loops. The value of H_s can be determined with high accuracy and is directly proportional to the uniaxial magnetic anisotropy, as shown in the following.

The in-plane free energy of a Co film on a stepped Cu(100) surface having the external magnetic field H applied along the $[110]$ direction is described by $K_u \sin^2(\phi) + K_1/4 \sin^2(2\phi) - \mu_0 H M_s \sin(\phi)$, where K_u and K_1 are the uniaxial and the cubic anisotropy constants, M_s the saturation magnetization, and ϕ the angle between the magnetization and the $[1\bar{1}0]$ direction [56]. Both K_u and K_1 are positive for the easy axis along $[1\bar{1}0]$. From an energy minimization with respect to ϕ and the approximation $K_u \ll K_1$, one finds that the uniaxial and the cubic anisotropies are given directly by the shift field H_s and the linear initial slope s of the loop, respectively: $K_u = \mu_0 H_s M_s$ and $K_1 = \mu_0 M_s^2 / 2s$. The assumption that K_u is small compared to K_1 is justified because the miscut of the Cu crystal—which induces the uniaxial anisotropy—is extremely small. Moreover, the hysteresis loops confirm the validity of the approximation because $H_s \approx 1 \text{ kA/m}$ is much smaller than $M_s / 2s \approx 50 \text{ kA/m}$ for all thicknesses $d > 2 \text{ ML}$. Note that we obtain no absolute values for M_s with the Kerr effect, because the magneto-optical constants are unknown. In order to determine magnetic anisotropies we must therefore rely on known M_s values. In the case of Co on Cu(100), $M_s = 1424 \text{ kA/m}$ regardless of thickness [57].

The initial slope s is experimentally more difficult to determine. For hysteresis loops such as the one presented in **Figure 7(b)**, no linear region between the shifted loops can be identified because the width of the loops is comparable to H_s . We can realize magnetization curves with an extended linear slope between the shifted loops by applying a constant bias field H_{bias} along the easy axis while sweeping the loop along the intermediate axis. The bias field introduces an additional unidirectional anisotropy, which results in a shift field of the two loops increased by H_{bias} . From the wide hysteresis-free field region between the loops we can now determine the initial slope s [see **Figure 7(c)**]. Note that the application of a bias field has a profound physical justification. The bias field forces the magnetization into the easy direction as soon as the sweeping field along the intermediate axis is reduced to zero, whereby a single-domain configuration is maintained. The increasing field along the intermediate axis then starts to tilt the magnetization reversibly away from the easy axis. This tilt angle is measured directly by

determining the magnetization component along the intermediate axis or, in other words, by determining the initial slope of the hysteresis loops. It signifies the anisotropy barrier against which the magnetization has to be rotated.

◆ *Morphology-induced anisotropy oscillations in Co/Cu(100)*
 Magnetic anisotropies of ultrathin films are inherently connected to the structure and morphology of the films. This has been shown, for example, for Ni/Cu(100) [58] and Co/Cu(110) [59]. In these systems strong relaxations of the lattice constants upon growth are found, giving rise to altered magnetic anisotropies. In principle the change of morphology associated with the change from a filled to an incompletely filled layer could also cause the magnetic anisotropy to change. Thus, provided the film grows layer by layer, one can envisage that the variations of the film roughness could lead to oscillations of the magnetic anisotropy with a period of 1 ML—analogous to the intensity variations in a reflection high-energy electron diffraction (RHEED) experiment.

Figure 8 presents the analysis in terms of anisotropy fields of transverse Kerr hysteresis loops taken during film growth. A bias field of 5 kA/m has been applied to determine both uniaxial and cubic anisotropy from the loop series as described in the preceding section. With increasing Co thickness d , the shift field $H_s(d)$ oscillates with a period of 1 ML, with minima at each completed layer, up to $d = 15$ ML [see Figure 8(a)]. The oscillation amplitude is damped with increasing d , which hints at a surface origin of the oscillations. On the other hand, no oscillations of the cubic anisotropy are observed within the somewhat larger uncertainty of fitting the initial slope of the loops [see Figure 8(b)]. We can exclude oscillations having an amplitude larger than 5% of the signal for $d > 5$ ML. Thus, oscillations having a relative amplitude comparable to the H_s oscillations are not present in M_s/s nor, hence, in K_1 . From additional experiments to determine K_1 more precisely, we can set an upper limit for the oscillation amplitude over the entire thickness range investigated, $\Delta K_1 < 1 \times 10^3 \text{ J/m}^3$.

Oscillations with a period of 1 ML have also been observed in Fe/Pd(100) superlattices with varying Pd thickness [60] in the coercive field H_c and have been attributed to a possible roughness modulation during the growth of successive Pd layers. The relation of coercive field to anisotropy is not straightforward, however, because H_c is determined by several physical mechanisms such as domain wall nucleation and pinning. Now, with the evidence of anisotropy oscillations, we can directly relate the two observations by also determining H_c from our loop series.

Figure 8(c) displays the half width of one of the shifted loops. As it corresponds to the coercive field of the easy-

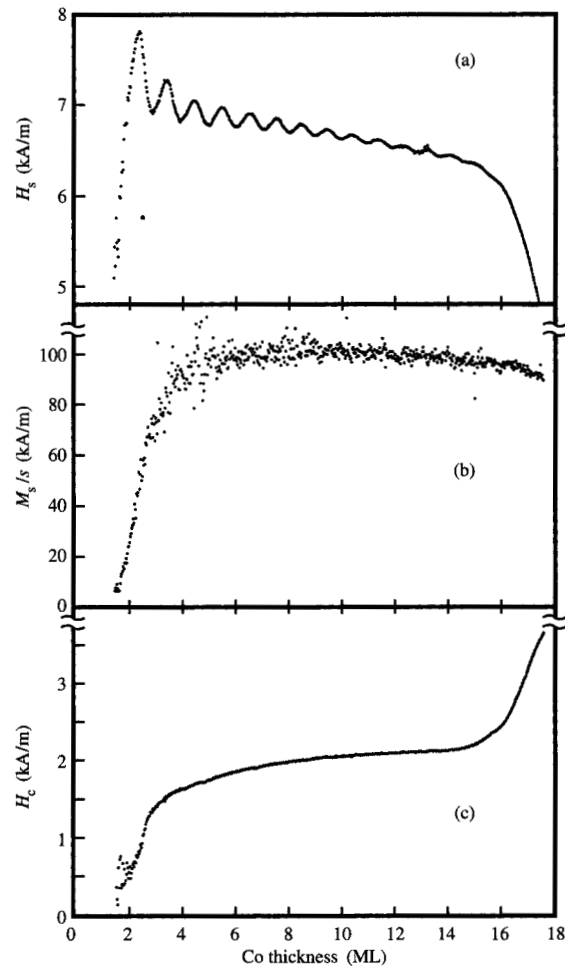


Figure 8

Analysis of transverse Kerr hysteresis loops taken during growth of a Co film on the stepped Cu(100) substrate as a function of Co thickness: (a) Shift field H_s , (b) inverse linear initial slope M_s/s , and (c) half width of one of the shifted loops H_c . A bias field of $H_{\text{bias}} = 5$ kA/m has been applied along the easy direction. The onset of ferromagnetism occurs at $d \approx 1.5$ ML at the measuring temperature of 320 K. The changes around 16 ML are accompanied by a structural relaxation of the Co film.

axis loop, we denote it as H_c . Like the shift field, $H_c(d)$ also reveals oscillations [10]. Their amplitudes are much smaller than for H_s and are clearly visible only after subtraction of a monotonously increasing smooth background curve. We conclude that the tiny oscillations in H_c are a consequence of the anisotropy changes. Obviously the latter are very weakly reflected in H_c .

What is the origin of the oscillations observed in the uniaxial anisotropy? The observation of a 1-ML period indicates a structural origin of the oscillations. In

principle, quantum size effects could also be responsible for anisotropy oscillations (see the subsection on magnetic anisotropy) because they periodically change the electronic band structure of the Co layer [13]. However, a period induced by quantum size effects is very unlikely to coincide accidentally with the lattice constant. Moreover, in the case of a period slightly different from 1 ML, one would expect to observe a phase slip at some Co thickness to accommodate the discreteness of the lattice, which is not observed in our experiment up to 15 ML.

From STM experiments it is known that Co on Cu(100) grows layer by layer above the first two monolayers [61]. As soon as a layer is completed, islands form in the next layer until they coalesce to a complete layer again. This means that the film morphology periodically changes from "flat" to "rough," corresponding to a complete and an incomplete top layer, respectively. The film roughness therefore oscillates with a period of 1 ML, as observed both by RHEED [62] and STM.

Evaporation in normal incidence onto a perfectly oriented Cu(100) surface yields on average Co patches with fourfold symmetry and step edges running along [110] and $[\bar{1}\bar{1}0]$ directions. The presence of steps in the Cu substrate, however, locally breaks the symmetry. This can result in rectangular rather than square Co islands owing to an anisotropic step-edge diffusion of the Co atoms [63]. Symmetry breaking can also directly influence the magnetic anisotropy at the step edges, which determines the observed macroscopic uniaxial anisotropy [55]. The excess length of one step direction compared to the orthogonal direction determines the anisotropy in the first case, the difference of local step anisotropies in the latter. To account for our observations, at least one of these quantities must be nonvanishing on our slightly miscut substrate, and thus varies during growth of the film. As soon as the layer is completed, it is minimized, resulting in an oscillatory variation of the uniaxial anisotropy.

Recent experiments obtained on Co/Cu(100) films by means of RHEED [62] might afford microscopic insight into the origin of magnetic step anisotropy. These experiments have shown that at the island edges of the incompletely filled top layer, the in-plane atomic spacing is different from that of completed layers. This results in an oscillatory variation of the average surface in-plane lattice spacing with film thickness. One can expect this change in atomic spacing at the island edges to produce magnetoelastic anisotropy.

Let us take a look at the fourfold anisotropy contribution. For symmetry reasons, contributions to the cubic in-plane anisotropy can only be expected to be of higher order because the uniaxial anisotropies of two edge atoms, located at orthogonal steps, compensate each other, yielding an isotropic instead of a fourfold symmetric situation. Taking this into account, a rough estimate of the

expected change of the fourfold anisotropy reveals that it is too small to be sensed in our experiment. With analogous reasoning, on the other hand, we can expect that the perpendicular surface anisotropy should also vary in an oscillatory fashion. Experimentally this might be more difficult to prove, because this would rely on the inherently inaccurate determination of an initial slope in the same way as for the cubic in-plane anisotropy.

In Figure 8 we see that both H_s and H_c exhibit a pronounced change in their overall course above ≈ 16 ML. In particular, H_s drops below $H_{\text{bias}} = 5$ kA/m, i.e., K_u changes sign. The easy magnetization axis flips from the $[\bar{1}\bar{1}0]$ to the $[110]$ direction at a critical thickness of $d_c = 16$ ML. A comparison with RHEED experiments provides strong evidence that these anisotropy changes are correlated with the onset of relaxation of the misfit-induced strain in the Co lattice upon growth [64].

This change of the easy magnetization axis by 90° within the plane might open the possibility of fabricating magnetoresistive read heads without the need for an additional biasing scheme. We discuss this topic briefly in the following paragraphs.

A useful sensor based on the giant magnetoresistance effect requires two magnetic layers in a single domain state separated by a nonmagnetic spacer material. The magnetization in the "pinned" layer must be fixed along a certain direction, whereas the magnetization of the "free" layer follows the magnetic field to be sensed, thus changing from more parallel to more antiparallel alignment with respect to the pinned layer when sensing two oppositely oriented bits. For linear operation of the device in an applied field, the magnetization of the two layers must be at an angle of 90° as long as no magnetic field is present. In the devices currently used, this "biasing" is achieved by fixing the magnetization of the pinned layer along its hard magnetization direction either by permanent magnets or by exchange coupling to an AF layer such as FeMn.

On the basis of Figure 8, an alternative way to achieve the required 90° orientation might become possible without the need for external biasing, exploiting the fact that the intrinsic easy magnetization direction as well as the coercive field depends strongly on film thickness [65]. As the coercive field increases strongly above d_c (it reaches values above 6 kA/m for the largest thicknesses investigated [64]), a thick Co layer keeps its magnetization aligned perpendicular to the step direction even in the external fields to be sensed and hence remains pinned. The small coercive field of a thin Co layer with $d < d_c$ should make such a film suitable as the free field-sensing layer. The magnetization directions of these films are orthogonal to each other without extrinsic biasing. The magnetic properties of the single films are also preserved in a test structure consisting of the two films separated by

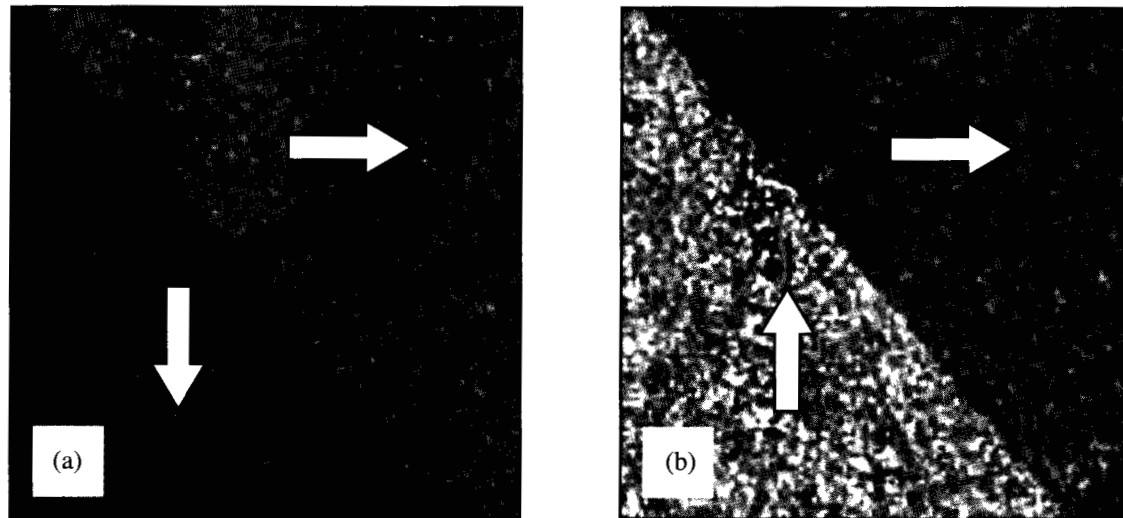


Figure 9

Magnetization image of a Co/Cu/Co/Cu(100) layered test structure that illustrates the principle of an unbiased magnetoresistive sensor acquired by spin-SEM. The stepped Cu(100) substrate is miscut by 1.6° . Thicknesses of the Co layers are 5 and 30 ML; thickness of the Cu layer is 100 ML. The upper right part of the square exposes the lower pinned Co layer, the lower left part the completed structure with the free overlying Co layer. Magnetization direction is indicated by arrows. Single domain remanent state (a) before and (b) after application of an external field pulse of 3 kA/m to invert the free layer.

a nonmagnetic spacer material, which decouples the films.

Figure 9 shows the magnetization image of a Co/Cu/Co/Cu(100)-layered structure, with $d = 5$ ML for the free Co layer, $d = 30$ ML for the pinned Co layer, and a Cu spacer thickness of 100 ML. The magnetization directions correspond to the easy axes of the single films and subtend an angle of 90° . An external magnetic field larger than the coercive field of the free layer switches the free layer but has no influence on the pinned layer [see Figure 9(b)]. We stress that both layers remain in a single domain state.

To obtain a working magnetoresistive device, the metallic Cu(100) substrate must be replaced by an insulating or semiconducting material. For instance, Si(100) could serve as a substrate for epitaxially grown or sputtered films of Co/Cu [66, 67], or MgO(100) [68].

• *Oscillations in Cu/Co/Cu(100) induced by quantum size effects*

Magneto-optical response

Oscillations of the magneto-optical response as a function of film thickness are currently attracting much interest [6–9]. Analogous to exchange-coupling oscillations, the

non-monotonous behavior of the magneto-optical response is also believed to be caused by a quantum size effect, which changes the electronic band structure periodically upon film growth. In particular, the occurrence of QW states is most likely responsible for the oscillatory behavior of the magneto-optical response [69]. As the overlayer thickness changes, the energetic positions of the QW states vary. If the corresponding bulk band crosses the Fermi level, QW states disperse through the Fermi level as a function of overlayer thickness. This results in a periodically changing occupied electronic band structure, which will be reflected in the magneto-optical response. Although both exchange and Kerr intensity oscillations can be interpreted as a quantum size effect, they generally exhibit different periodicities. To determine the exchange-coupling oscillations, the stationary spanning vectors of the Fermi surface have to be considered. To determine the period of the magneto-optical oscillations, on the other hand, consideration must be given to those occupied and empty states around the Fermi level that are separated by the photon energy and share the same wave vector.

We have investigated the magneto-optical response in Co/Cu(100) films during the growth of a Cu overlayer. A series of hysteresis loops was taken by the transverse Kerr effect, measured at a light wavelength of 633 nm

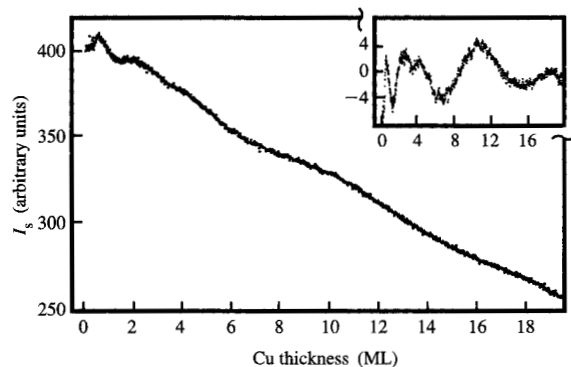


Figure 10

Saturation Kerr intensity I_s of a 5-ML-thick Co film on a 0.1° off-oriented Cu(100) crystal as a function of Cu coverage. The inset shows I_s after subtraction of a fitted exponential background.

(corresponding to a photon energy of 1.96 eV). From these loops, the saturation Kerr intensity I_s was determined as a function of the Cu overlayer thickness d_{Cu} [see **Figure 10**].

Up to $d_{\text{Cu}} = 0.5$ ML, I_s exhibits a slight increase, then drops sharply, and finally decreases slowly for $d_{\text{Cu}} > 1.2$ ML. Similar behavior has been observed before [70]. The overall decrease of the I_s curve above 1.2 ML is reconciled by the finite probing depth of the Kerr experiment. The sharp drop below $d_{\text{Cu}} = 1.2$ ML, on the other hand, must be of magneto-optical origin. The possibility of a drastic loss of the Co magnetic moment at the Co/Cu interface is ruled out as the cause for this observation on the basis of a determination of the spin polarization of the secondary electrons. A purely exponential decay of spin polarization is observed upon Cu coverage, indicating that the Co spin moment is not affected by the Cu coverage [see **Figure 5(a)**].

For $d_{\text{Cu}} > 1.2$ ML, we observe oscillations in I_s superimposed on the exponential background, with peaks located near 2.5, 4, 10, and 18 ML. Interestingly, a recent study of Cu/Co(100) did not detect oscillations in the magneto-optical response but found peaks in the second-harmonics signal [9]. Additional Kerr experiments up to $d_{\text{Cu}} = 50$ ML reveal the existence of further broad I_s structures at $d_{\text{Cu}} \approx 30$ and ≈ 40 ML. A unique period of the oscillations is difficult to determine. It is likely that a superposition of different periods exists, originating from different parts of the Brillouin zone. We attempt to identify these regions. The analogy between the exchange-coupling oscillations and the magneto-optical response suggests that spanning vectors at or near high-symmetry points of the Brillouin zone are stationary and hence

responsible for the periodicity observed. Therefore, we look for possible magneto-optical transitions at and near the $\bar{\Gamma}$ and \bar{X} points.

At both points, magneto-optical transitions with $\Delta E = 1.96$ eV are possible. The QW-state picture developed in Reference [13] relates the perpendicular wave vector components of the Brillouin zone boundary $k_{z\text{b}}$ and of the magneto-optical transition k_{\perp} to the expected period, $k_{\perp} = (1 - 1/\lambda)k_{z\text{b}}$. The period λ is given in ML and is 2–3 ML for the \bar{X} point and 6–9 ML for the $\bar{\Gamma}$ point. Calculations have shown that Cu-*s*, *p* minority-spin states at the \bar{X} point are much more strongly confined than at the $\bar{\Gamma}$ point and hence should more effectively contribute to the oscillations [19]. From the discrepancy between the observed peak differences and the estimated periods, however, we conclude that magneto-optical transitions near the $\bar{\Gamma}$ point are most likely responsible for the observed I_s oscillations.

Magnetic anisotropy

As the magnetic anisotropy is caused by the spin-orbit coupling of the electrons, it is closely connected to the relativistic electronic band structure. Thus, shifts in the energy and changes in the occupancy of electronic states can in principle affect the magnetic anisotropy. An attractive way to alter electronic states is to confine them to a small region, thereby quantizing their energy and wave vector. We have investigated the possibility that quantum confinement leads to periodic changes in the magnetic anisotropy of a ferromagnetic film with increasing layer thickness. Theoretically a periodic variation of the uniaxial magnetic anisotropy has been predicted [71], indicating that the surface anisotropy is not of purely local origin in the top atomic layer, but is also influenced, via quantum confinement, by atomic layers farther away from the surface.

For a precise determination of variations in the magnetic anisotropy, we again deposited Co films on the 0.1° off-oriented Cu(100) substrate to determine the anisotropy fields directly from the intermediate-axis hysteresis loops, as described earlier in Section 2. For these experiments a Co film of fixed thickness was deposited, followed by a Cu overlayer. Hysteresis loops were measured during the growth of the Cu film. The anisotropy fields deduced from each of these loops are given in **Figure 11** as a function of Cu thickness d_{Cu} . Remarkably, both the uniaxial and the cubic anisotropy of the Co film displayed a pronounced oscillatory variation with d_{Cu} .

At submonolayer coverages of Cu, a drastic decrease of H_s was found (see inset in **Figure 11**). It has been suggested elsewhere [55] that this first drop is caused by a decoration of the Co step atoms by the Cu adsorbate, which changes the electronic band structure at the step

atoms. In fact, chemically sensitive STM experiments prove that submonolayer coverages of Cu attach to Co step sites [72]. This anisotropy change appears for different adsorbates such as Cu, Ag, and O [73] and can even be strong enough to change the easy magnetization axis by 90° within the plane. For all adsorbates except Cu, H_s varies monotonously for coverages up to 3 ML.

A similar anomalous behavior of the magnetic anisotropy has also been observed in perpendicularly magnetized systems, e.g. in Co(111) films covered by Au, Cu, or Ag [74, 75]. It has been interpreted to arise from hybridization between Co and the overlayer electronic states. The maximum change of anisotropy, which is reached for adsorbate coverages of about 1 ML, seems to be related to the existence of interface states [76]. In our case of a stepped Co surface, hybridization at the step atom positions could be the mechanism responsible for the switching of the easy magnetization direction in the submonolayer coverage range. For the nonmetallic O coverage, however, hybridization cannot explain the observed effect because the required band overlap between Co and O is small.

For Cu overlayers, additional non-monotonous changes occur at larger thicknesses above 1 ML. An increase of H_s occurs, resulting in a maximum at $d_{\text{Cu}} = 1.2$ ML. Further maxima of H_s can be identified at $d_{\text{Cu}} = 4.1, \approx 7.7, \approx 12,$ and ≈ 16 ML. An approximate period of 3–4 ML can be deduced. Thus, structural changes as the origin of the oscillations can be ruled out immediately. In fact, we do not expect a morphology-induced 1-ML oscillation period for increasing d_{Cu} , as observed as a function of the Co film thickness [see the section on morphology-induced anisotropy oscillations in Co/Cu(100)], because the growth of the Cu layer does not affect the Cu/Co interface as soon as a few monolayers are completed. Thus, the magnetic surface anisotropy of the Co film is not affected. However, we cannot rule out that the observed anisotropy peaks are the result of a superposition of more than one period because the peak positions are not equidistant. Indeed, very recent measurements on Cu/Co/Cu(100) films, where the Cu overlayer was grown at low temperatures, give evidence that two periods exist [77]. The different growth of Cu on Co at low temperatures in comparison to room temperature is most likely the cause for the different oscillatory behavior. Interestingly, the periods are in good agreement with those found in exchange-coupling experiments [22, 50].

We note that the amplitudes at large Cu coverages are extremely small, being of the order of 1 A/m. The fourfold cubic anisotropy also shows oscillations with d_{Cu} [see Figure 11(b)]. The peaks of M_s/s are found at the same positions as observed for the uniaxial magnetic anisotropy, even though the overall curve is different. These observations show that the addition of Cu, i.e., the

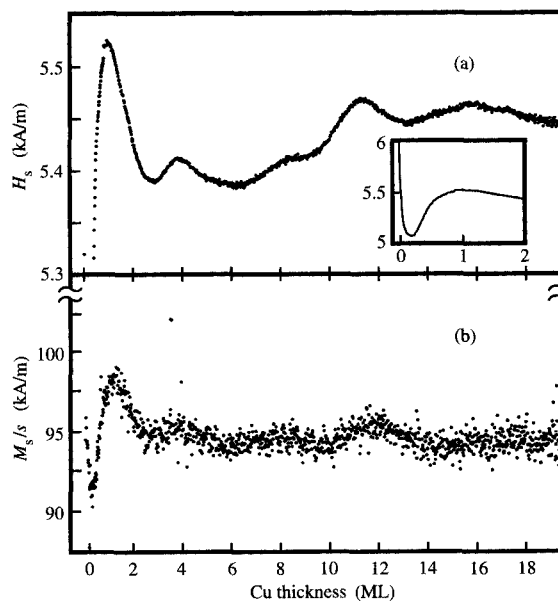


Figure 11

(a) Shift field H_s and (b) M_s/s of a 5-ML-thick Co film on a 0.1° off-oriented Cu(100) crystal as a function of the thickness of an overlying Cu film. A bias field of 5.3 kA/m has been applied. The inset in (a) shows the low-coverage region with a line through the data points to guide the eye. Adapted from [11] with permission.

displacement of the vacuum/Cu interface from the Co film, influences the magnetic anisotropy of the deeper-lying Co film in an oscillatory fashion, even if the Co film is separated by as much as 16 ML from the Cu/Co interface.

The good agreement between the periods of magnetic anisotropy and exchange coupling found by Würsch et al. [77] suggests that the behavior of the conduction electrons at the Fermi level is also most likely responsible for the magnetic anisotropy oscillations, as is the case for the exchange-coupling oscillations. The experimental observation that the uniaxial and the cubic anisotropies exhibit the same peak positions further indicates that only a very limited set of spin-orbit split electronic states is responsible for the main contribution to the oscillatory part of magnetic anisotropy.

If the observed anisotropy oscillations are induced by a quantum size effect in Cu, one expects them to be unaffected by Co thickness. We therefore repeated the experiment for different Co film thicknesses, i.e., for different initial shift fields and hence different strengths of the uniaxial anisotropy. We found that the positions of the anisotropy extrema are independent of the Co thickness [11]. Thus, the influence of the Cu overlayer on the

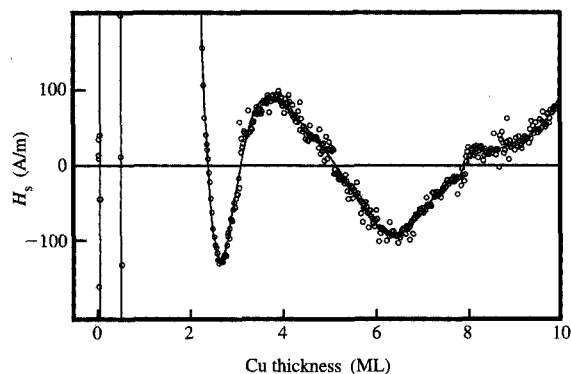


Figure 12

Shift field H_s vs. Cu coverage for a 10.8-ML Co film on a 3.4° off-oriented Cu(100) crystal. The initial shift field at $d_{\text{Cu}} = 0$ ML is $H_s = 9.3$ kA/m. Sign changes of H_s indicate that the easy axis switches repeatedly between the $[1\bar{1}0]$ and $[110]$ directions.

magnetic film is confined to the Co/Cu interface, as expected for a quantum size effect.

The ability to tailor the magnitude of the uniaxial anisotropy by choosing the appropriate Co film thickness offers fascinating prospects. For example, it allows us to fabricate a magnetic thin-film system in which the magnetization direction switches repeatedly between two well-defined states: from being parallel to the preferential step direction to being perpendicular to it. **Figure 12** shows as an example a 10.8-ML Co film grown on a Cu(100) single crystal miscut by 3.4° . The initial shift field present before the Cu overlayer is grown is small enough to be balanced by the adsorption of the first 0.05 ML of Cu. Further Cu coverage allows the easy magnetization direction to oscillate repeatedly between the $[1\bar{1}0]$ and the $[110]$ directions.

We note that the concept of quantum confinement loses its strict meaning for very thin layers, for which the notion of interface states is more appropriate. In this context, the observation of the anisotropy change or even the switching of the easy axis just above 0.3 ML Cu coverage can be taken as the evolution of an interface state or, in other words, as a precursor of quantum confinement at very small Cu coverage.

4. Concluding remarks

The discovery of oscillatory exchange coupling between two ferromagnets separated by a nonmagnetic metallic spacer has opened a broad field of research. Our understanding of the physical mechanisms underlying these oscillations has progressed, and the seemingly

different approaches of an RKKY model and a QW model have partly converged in the most recent theoretical approaches. The QW model features the intuitive interpretation of an electron wave confined in a small one-dimensional box, and this simple approach has led to experimental and theoretical investigations of possible oscillatory behavior of various other physical quantities apart from exchange coupling.

The intention of this overview has been to discuss several oscillatory magnetic properties for a particular model system. We have chosen epitaxial fcc Co films grown on Cu(100) as the basis for our experimental investigations and have selected additional epitaxial overlayers to study interlayer exchange coupling, induced magnetic moments, magneto-optical properties, and magnetic anisotropy.

We have found oscillations in all of these quantities. In Section 2 we described a comparative study of the exchange oscillations across a Cu spacer, and we have determined periods, amplitude ratios, and peak shifts of exchange-coupled films from spin-SEM images. The oscillation periods found for the model system Co/Cu/Co(100) agree very well with predictions of RKKY theory, and hence fully support the explanation of exchange coupling based on Fermi surface properties. The observed large amplitude ratio, however, cannot be explained within the RKKY model. Instead one must take into account the degree of band matching at the interfaces, a parameter contained in the most recent QW models. The most remarkable result of the exchange-coupling experiments is the peculiar behavior of the AF peak positions when one ferromagnet is substituted for another. Long- and short-period oscillations behave differently: Long-period oscillations are unaffected by a change in the ferromagnetic material, whereas short-period oscillations are influenced by it. This behavior can be understood as a consequence of the rather different degrees of confinement to which the electrons are subjected. The sign of the short-period peak shifts is in accordance with a simple theory, which takes band filling into account. The general trend of a disappearance of the peak shift for large Cu spacer thicknesses, however, cannot be understood in terms of existing theories.

Furthermore, in Section 2 we described a method to determine the oscillatory spin density, which mediates the coupling between the ferromagnetic layers. For that purpose, we replaced the top ferromagnetic layer with a paramagnetic layer having a very high susceptibility, namely fcc Fe above its magnetic ordering temperature.

In Section 3 we covered oscillations of the magneto-optical response and of the magnetic anisotropy, as measured by a careful analysis of Kerr hysteresis loops. For the stepped Co/Cu(100) system, oscillations of the uniaxial magnetic anisotropy with a periodicity of 1 ML

are found. By comparison with results of structural investigations, these oscillations can be ascribed to the periodic change of the film morphology from "rough" to "flat" upon growth when the atomic layers become filled. The Cu/Co/Cu system, on the other hand, exhibits oscillations of a different origin. Both the uniaxial and the cubic magnetic anisotropy show a period that is larger than but not a multiple of 1 ML. This excludes morphological changes upon Cu growth as the origin of the oscillations. Instead, quantum confinement is the most likely explanation for the oscillatory behavior of the anisotropy. Interestingly, oscillations of the magneto-optical response are also observed in this system, but their period is different from that of both the anisotropy oscillations and the exchange oscillations across Cu(100), as discussed in Section 2. Thus, for the particular model system of a Cu(100) spacer layer, four different magnetic quantities have been found to oscillate—exchange coupling, induced magnetic moment, magnetic anisotropy, and the magneto-optical response. All of these types of oscillations can be explained in terms of quantum confinement within the Cu layer.

It is intriguing to speculate that other magnetic properties might also show oscillations not yet identified in these high-quality epitaxial structures.

Acknowledgments

We are grateful to Ch. Würsch, C. Stamm, S. Egger, and D. Pescia for communicating their unpublished results to us.

References

1. C. F. Majkrzak, J. W. Cable, J. Kwo, M. Hong, D. B. McWhan, Y. Yafet, J. V. Waszczak, and C. Vettier, "Observation of a Magnetic Antiphase Domain Structure with Long-Range Order in a Synthetic Gd-Y Superlattice," *Phys. Rev. Lett.* **56**, 2700–2703 (1986).
2. J. Kwo, M. Hong, F. J. DiSalvo, J. V. Waszczak, and C. F. Majkrzak, "Modulated Magnetic Properties in Synthetic Rare-Earth Gd-Y Superlattices," *Phys. Rev. B* **35**, 7295–7298 (1987).
3. S. S. P. Parkin, N. More, and K. P. Roche, "Oscillations in Exchange Coupling and Magnetoresistance in Metallic Superlattice Structures: Co/Ru, Co/Cr, and Fe/Cr," *Phys. Rev. Lett.* **64**, 2304–2307 (1990).
4. M. N. Baibich, J. M. Broto, A. Fert, F. Nguyen Van Dau, F. Petroff, P. Etienne, G. Creuzet, A. Friederich, and J. Chazelas, "Giant Magnetoresistance of (001)Fe/(001)Cr Magnetic Superlattices," *Phys. Rev. Lett.* **61**, 2472–2475 (1988).
5. G. Binash, P. Grünberg, F. Saurenbach, and W. Zinn, "Enhanced Magnetoresistance in Layered Magnetic Structures with Antiferromagnetic Interlayer Exchange," *Phys. Rev. B* **39**, 4828–4830 (1989).
6. W. Geerts, Y. Suzuki, T. Katayama, K. Ando, and S. Yoshida, "Thickness-Dependent Oscillation of the Magneto-Optical Properties of Au-Sandwiched (001) Fe Films," *Phys. Rev. B* **50**, 12581–12586 (1994).
7. R. Mégy, A. Bounouh, Y. Suzuki, P. Beauvillain, P. Bruno, C. Chappert, B. Lecuyer, and P. Veillet, "Magneto-Optical-Kerr-Effect Study of Spin Polarized Quantum Well States in a Au Overlay on a Co(0001) Ultrathin Film," *Phys. Rev. B* **51**, 5586–5589 (1995).
8. A. Carl and D. Weller, "Oscillatory Paramagnetic Magneto-Optical Kerr Effect in Ru Wedges on Co," *Phys. Rev. Lett.* **74**, 190–193 (1995).
9. H. A. Wierenga, W. de Jong, M. W. J. Prins, Th. Rasing, R. Vollmer, A. Kirilyuk, H. Schwabe, and J. Kirschner, "Interface Magnetism and Possible Quantum Well Oscillations in Ultrathin Co/Cu Films Observed by Magnetization Induced Second Harmonic Generation," *Phys. Rev. Lett.* **74**, 1462–1465 (1995).
10. W. Weber, C. H. Back, A. Bischof, Ch. Würsch, and R. Allenspach, "Morphology-Induced Oscillations of the Magnetic Anisotropy in Ultrathin Co Films," *Phys. Rev. Lett.* **76**, 1940–1943 (1996).
11. W. Weber, A. Bischof, R. Allenspach, Ch. Würsch, C. H. Back, and D. Pescia, "Oscillatory Magnetic Anisotropy and Quantum Well States in Cu/Co/Cu(100) Films," *Phys. Rev. Lett.* **76**, 3424–3427 (1996).
12. T. Miller, A. Samsavar, G. E. Franklin, and T.-C. Chiang, "Quantum-Well States in a Metallic System: Ag on Au(111)," *Phys. Rev. Lett.* **61**, 1404–1407 (1988).
13. J. E. Ortega, F. J. Himpsel, G. J. Mankey, and R. F. Willis, "Quantum-Well States and Magnetic Coupling Between Ferromagnets Through a Noble-Metal Layer," *Phys. Rev. B* **47**, 1540–1552 (1993).
14. K. Garrison, Y. Chang, and P. D. Johnson, "Spin Polarization of Quantum Well States in Copper Thin Films Deposited on a Co(001) Substrate," *Phys. Rev. Lett.* **71**, 2801–2804 (1993).
15. C. Carbone, E. Vescovo, O. Rader, W. Gudat, and W. Eberhardt, "Exchange-Split Quantum Well States of a Noble Metal Film on a Magnetic Substrate," *Phys. Rev. Lett.* **71**, 2805–2808 (1993).
16. P. Grünberg, R. Schreiber, Y. Pang, M. B. Brodsky, and H. Sowers, "Layered Magnetic Structures: Evidence for Antiferromagnetic Coupling of Fe Layers Across Cr Interlayers," *Phys. Rev. Lett.* **57**, 2442–2445 (1986).
17. S. S. P. Parkin, "Systematic Variation of the Strength and Oscillation Period of Indirect Magnetic Exchange Coupling Through 3d, 4d, and 5d Transition Metals," *Phys. Rev. Lett.* **67**, 3598–3601 (1991).
18. D. M. Edwards, J. Mathon, R. B. Muniz, and M. S. Phan, "Oscillations of the Exchange in Magnetic Multilayers as an Analog of de Haas-van Alphen Effect," *Phys. Rev. Lett.* **67**, 493–496 (1991).
19. P. Lang, L. Nordström, R. Zeller, and P. H. Dederichs, "Ab Initio Calculations of the Exchange Coupling of Fe and Co Monolayers in Cu," *Phys. Rev. Lett.* **71**, 1927–1930 (1993); L. Nordström, P. Lang, R. Zeller, and P. H. Dederichs, "Influence of the Magnetic-Layer Thickness on the Interlayer Exchange Coupling: Competition Between Oscillation Periods," *Phys. Rev. B* **50**, 13058–13061 (1994).
20. R. Coehoorn, "Period of Oscillatory Exchange Interactions in Co/Cu and Fe/Cu Multilayer Systems," *Phys. Rev. B* **44**, 9331–9337 (1991).
21. P. Bruno and C. Chappert, "Oscillatory Coupling Between Ferromagnetic Layers Separated by a Nonmagnetic Metal Spacer," *Phys. Rev. Lett.* **67**, 1602–1605, 2592 (1991); P. Bruno and C. Chappert, "Ruderman-Kittel Theory of Oscillatory Interlayer Exchange Coupling," *Phys. Rev. B* **46**, 261–270 (1992).
22. M. T. Johnson, S. T. Purcell, N. W. E. McGee, R. Coehoorn, J. aan de Stegge, and W. Hoving, "Structural Dependence of the Oscillatory Exchange Interaction Across Cu Layers," *Phys. Rev. Lett.* **68**, 2688–2691 (1992).
23. P. J. H. Bloemen, M. T. Johnson, M. T. H. van de Vorst, R. Coehoorn, J. J. de Vries, R. Jungblut, J. aan de Stegge, A. Reinders, and W. J. M. de Jonge, "Magnetic Layer Thickness Dependence of the Interlayer Exchange Coupling in (001) Co/Cu/Co," *Phys. Rev. Lett.* **72**, 764–767 (1994).

24. J. J. de Vries, A. A. P. Schudelaro, R. Jungblut, P. J. H. Bloemen, A. Reinders, J. Kohlhepp, R. Coehoorn, and W. J. M. de Jonge, "Oscillatory Interlayer Exchange Coupling with the Cu Cap Layer Thickness in Co/Cu/Co/Cu(100)," *Phys. Rev. Lett.* **75**, 4306-4309 (1995).
25. J. Barnas, "Coupling Between Two Ferromagnetic Films Through a Non-Magnetic Metallic Layer," *J. Magn. Magn. Mater.* **111**, L215-219 (1992).
26. P. Bruno, "Oscillations of Interlayer Exchange Coupling vs. Ferromagnetic-Layers," *Europhys. Lett.* **23**, 615-620 (1993).
27. P. Lang, L. Nordström, K. Wildberger, R. Zeller, and P. H. Dederichs, "Ab Initio Calculations of Interaction Energies of Magnetic Layers in Noble Metals: Co/Cu(100)," *Phys. Rev. B* **53**, 9092-9107 (1996).
28. J. Mathon, M. Villeret, M. B. Muniz, J. d'Albuquerque e Castro, and D. M. Edwards, "Quantum Well Theory of the Exchange Coupling in Co/Cu/Co(001)," *Phys. Rev. Lett.* **74**, 3696-3699 (1995).
29. B. Lee and Y.-Ch. Chang, "Effects of Realistic Band Structures on the Interlayer Coupling Strengths in Magnetic Multilayers," *Phys. Rev. B* **52**, 3499-3510 (1995).
30. R. Coehoorn, A. De Veirman, and J. P. W. B. Duchateau, "The Phase of the Oscillatory Exchange Coupling in Coherent fcc (Fe-Co-Ni)/Cu(001) Multilayers," *J. Magn. Magn. Mater.* **121**, 266-269 (1993).
31. M. T. Johnson, M. T. H. van de Vorst, P. J. H. Bloemen, R. Coehoorn, A. Reinders, J. aan de Stegge, and R. Jungblut, "Phase Shifts in the Oscillatory Interlayer Exchange Coupling Across Cu Layers," *Phys. Rev. Lett.* **75**, 4686-4689 (1995).
32. H. Matsuyama and K. Koike, "A Data Acquisition and Display System for Spin-Polarized Scanning Electron Microscopy (Spin SEM)," *Rev. Sci. Instrum.* **62**, 970-981 (1991).
33. J. Unguris, R. J. Celotta, and D. T. Pierce, "Observation of Two Different Oscillation Periods in the Exchange Coupling of Fe/Cr/Fe(100)," *Phys. Rev. Lett.* **67**, 140-143 (1991).
34. R. Allenspach, "Ultrathin Films: Magnetism on the Microscopic Scale," *J. Magn. Magn. Mater.* **129**, 160-185 (1994).
35. R. Allenspach, A. Bischof, M. Stampanoni, D. Kerkmann, and D. Pescia, "Growing Thin Magnetic Films with a Mask: Distinguishing Between Magnetic and Instrumental Asymmetries," *Appl. Phys. Lett.* **60**, 1908-1910 (1992).
36. C. H. Back, W. Weber, A. Bischof, D. Pescia, and R. Allenspach, "Probing Oscillatory Exchange Coupling with a Paramagnet," *Phys. Rev. B* **52**, R13114-R13117 (1995).
37. A. Cebollada, R. Miranda, C. M. Schneider, P. Schuster, and J. Kirschner, "Experimental Evidence of an Oscillatory Magnetic Coupling in Co/Cu/Co Epitaxial Layers," *J. Magn. Magn. Mater.* **102**, 25-29 (1991).
38. Z. Q. Qiu, J. Pearson, and S. D. Bader, "Oscillatory Interlayer Magnetic Coupling of Wedged Co/Cu/Co Sandwiches Grown on Cu(100) by Molecular Beam Epitaxy," *Phys. Rev. B* **46**, 8659-8662 (1992).
39. P. J. H. Bloemen, R. van Dalen, W. J. M. de Jonge, M. T. Johnson, and J. aan de Stegge, "Short Period Oscillation of the Interlayer Exchange Coupling in the Ferromagnetic Regime in Co/Cu/Co(100)," *J. Appl. Phys.* **73**, 5972-5974 (1993).
40. J. Unguris, R. J. Celotta, and D. T. Pierce, "Oscillatory Magnetic Coupling in Fe/Ag/Fe(100) Sandwich Structures," *J. Magn. Magn. Mater.* **127**, 205-213 (1993).
41. P. Bruno, "Physical Mechanism of Oscillatory Interlayer Exchange Coupling," *J. Magn. Magn. Mater.* **116**, L13-17 (1992); P. Bruno, "Interlayer Exchange Coupling: A Unified Physical Picture," *ibid.* **121**, 248-252 (1993).
42. D. D. Chambliss, R. J. Wilson, and S. Chiang, "Nucleation and Growth of Ultrathin Fe and Au Films on Cu(100) Studied by Scanning Tunneling Microscopy," *J. Vac. Sci. Technol. A* **10**, 1993-1998 (1992).
43. J. Fassbender, R. Allenspach, and U. Dürig, "Intermixing and Growth Kinetics of the First Co Monolayers on Cu(001)," *Surf. Sci.* **383**, L742-L748 (1997).
44. M. G. Samant, J. Stöhr, S. S. P. Parkin, G. A. Held, B. D. Hermsmeier, F. Herman, M. van Schilfgaarde, L.-C. Duda, D. C. Mancini, N. Wassdahl, and R. Nakajima, "Induced Spin Polarization in Cu Spacer Layers in Co/Cu Multilayers," *Phys. Rev. Lett.* **72**, 1112-1115 (1994).
45. See for example G. A. Mulhollan, R. L. Fink, J. L. Erskine, and G. K. Walters, "Local Spin Correlations in Ultrathin Fe/W(100) Films," *Phys. Rev. B* **43**, 13645-13648 (1991); D. Kerkmann, D. Pescia, and R. Allenspach, "Two-Dimensional Magnet at Curie Temperature: Epitaxial Layers of Co on Cu(100)," *Phys. Rev. Lett.* **68**, 686-689 (1992); M. Farle, K. Baberschke, U. Stetter, A. Aspelmeier, and F. Gerhardt, "Thickness-Dependent Curie Temperature of Gd(0001)/W(11) and Its Dependence on the Growth Conditions," *Phys. Rev. B* **47**, 11571-11574 (1993); C. H. Back, C. Würsch, D. Kerkmann, and D. Pescia, "Giant Magnetic Susceptibility in Fe and Co Epitaxial Films," *Z. Phys. B* **96**, 1-3 (1994).
46. E. J. Escorcia-Aparicio, R. K. Kawakami, and Z. Q. Qiu, "fcc Fe Films Grown on a Ferromagnetic fcc Co(100) Substrate," *Phys. Rev. B* **54**, 4155-4158 (1996).
47. S. F. Alvarado, R. Feder, H. Hopster, F. Ciccacci, and H. Pleyer, "Simultaneous Probing of Exchange and Spin-Orbit Interaction in Spin Polarized Low Energy Electron Diffraction from Magnetic Surfaces," *Z. Phys. B* **49**, 129-132 (1982).
48. E. R. Moog, C. Liu, S. D. Bader, and J. Zak, "Thickness and Polarization Dependence of the Magneto-optical Signal from Ultrathin Ferromagnetic Films," *Phys. Rev. B* **39**, 6949-6956 (1989).
49. K. Koike, T. Furukawa, G. P. Cameron, and Y. Murayama, "Intensity and Polarization Oscillation of Secondary Electrons Emitted from Au/Fe(110)," *Phys. Rev. B* **50**, 4816-4818 (1994).
50. W. Weber, R. Allenspach, and A. Bischof, "Exchange Coupling Across Cu(100): A High-Precision Study," *Europhys. Lett.* **31**, 491-496 (1995); *ibid.* **32**, 379 (1995).
51. H. J. Elmers, T. Furubayashi, M. Albrecht, and U. Gradmann, "Analysis of Magnetic Anisotropies in Ultrathin Films by Magnetometry In Situ in UHV," *J. Appl. Phys.* **70**, 5764-5768 (1991).
52. B. Heinrich, J. F. Cochran, A. S. Arrott, S. T. Purcell, K. B. Urquhart, J. R. Dutcher, and W. F. Egelhoff, Jr., "Development of Magnetic Anisotropies in Ultrathin Epitaxial Films of Fe(001) and Ni(001)," *Appl. Phys. A* **49**, 473-490 (1989).
53. A. Berger, U. Linke, and H. P. Oepen, "Symmetry-Induced Uniaxial Anisotropy in Ultrathin Epitaxial Cobalt Films on Cu(1 1 13)," *Phys. Rev. Lett.* **68**, 839-842 (1992).
54. P. Krams, B. Hillebrands, G. Güntherodt, and H. P. Oepen, "Magnetic Anisotropies of Ultrathin Co Films on Cu(1 1 13) Substrates," *Phys. Rev. B* **49**, 3633-3636 (1994).
55. W. Weber, C. H. Back, A. Bischof, D. Pescia, and R. Allenspach, "Magnetic Switching in Cobalt Films by Adsorption of Copper," *Nature* **374**, 788-790 (1995).
56. H. P. Oepen, C. M. Schneider, D. S. Chuang, C. A. Ballentine, and R. C. O'Handley, "Magnetic Anisotropy in Epitaxial fcc Co/Cu(1 1 13)," *J. Appl. Phys.* **73**, 6186-6188 (1993).
57. P. Krams, F. Lauks, R. L. Stamps, B. Hillebrands, and G. Güntherodt, "Magnetic Anisotropies of Ultrathin Co(001) Films on Cu(001)," *Phys. Rev. Lett.* **69**, 3674-3677 (1992).

58. R. Jungblut, M. T. Johnson, J. aan de Stegge, A. Reinders, and F. J. A. den Broeder, "Orientational and Structural Dependence of Magnetic Anisotropy of Cu/Ni/Cu Sandwiches: Misfit Interface Anisotropy," *J. Appl. Phys.* **75**, 6424-6426 (1994).
59. J. Fassbender, C. Mathieu, B. Hillebrands, G. Güntherodt, R. Jungblut, and M. T. Johnson, "Identification of Magnetocrystalline and Magnetoelastic Anisotropy Contributions in Ultrathin Epitaxial Co(110) Films," *J. Magn. Magn. Mater.* **148**, 156-157 (1995).
60. J. R. Childress, R. Kergoat, O. Durand, J.-M. George, P. Galtier, J. Miltat, and A. Schuhl, "Magnetic Properties and Domain Structure of Epitaxial (001)Fe/Pd Superlattices," *J. Magn. Magn. Mater.* **130**, 13-22 (1994).
61. A. K. Schmid and J. Kirschner, "In Situ Observation of Epitaxial Growth of Co Thin Films on Cu(100)," *Ultramicrosc.* **42-44**, 483-489 (1992).
62. J. Fassbender, U. May, B. Schirmer, R. M. Jungblut, B. Hillebrands, and G. Güntherodt, "Oscillatory Surface In-Plane Lattice Spacing During Growth of Co and of Cu on a Cu(001) Single Crystal," *Phys. Rev. Lett.* **75**, 4476-4479 (1995).
63. J. Cousty, R. Peix, and B. Perrailon, "Diffusion Superficielle sur le Cuivre: Influence des Marches," *Surf. Sci.* **107**, 586-604 (1981).
64. W. Weber, A. Bischof, R. Allenspach, C. H. Back, J. Fassbender, U. May, B. Schirmer, R. M. Jungblut, G. Güntherodt, and B. Hillebrands, "Structural Relaxation and Magnetic Anisotropy in Co/Cu(001) Films," *Phys. Rev. B* **54**, 4075-4079 (1996).
65. R. Allenspach and W. Weber, "Magnetoresistive Sensor," PCT Patent Application WO 96/16339, 1996.
66. S. K. J. Lenczowski, M. A. M. Gijs, J. B. Giesbers, R. J. M. van de Veerdonk, and W. J. M. de Jonge, "Interpretation of the Giant Magnetoresistance Effect in Co/Cu(100) Multilayers with the Quantum Model of Giant Magnetoresistance," *Phys. Rev. B* **50**, 9982-9988 (1994).
67. Chin-An Chang, "Magnetocrystalline Anisotropy of (100) Face-Centered Cubic Co Structures Deposited on Cu/Si(100)," *Appl. Phys. Lett.* **58**, 1745-1747 (1991).
68. G. R. Harp and S. S. P. Parkin, "Seeded Epitaxy of Metals by Sputter Deposition," *Appl. Phys. Lett.* **65**, 3063-3065 (1994).
69. P. Bruno, Y. Suzuki, and C. Chappert, "Magneto-Optical Kerr Effect in a Paramagnetic Overlayer on a Ferromagnetic Substrate: A Spin-Polarized Quantum Size Effect," *Phys. Rev. B* **53**, 9214-9220 (1996).
70. M. E. Buckley, F. O. Schumann, and J. A. C. Bland, "Strong Changes in the Magnetic Properties of Ultrathin Co/Cu(001) Films Due to Submonolayer Quantities of a Nonmagnetic Overlayer," *Phys. Rev. B* **52**, 6596-6605 (1995).
71. M. Cinal, D. M. Edwards, and J. Mathon, "Magnetocrystalline Anisotropy in Ferromagnetic Films," *Phys. Rev. B* **50**, 3754-3760 (1994); "Magnetocrystalline Anisotropy in (110) fcc Cobalt Films," *J. Magn. Magn. Mater.* **140-144**, 681-682 (1995).
72. R. Allenspach, A. Bischof, and U. Dürig, "Cu Adsorption on Co Films: Edge Decoration Versus Intermixing," *Surf. Sci.* **381**, L573-L580 (1997).
73. W. Weber, C. H. Back, U. Ramsperger, A. Vaterlaus, and R. Allenspach, "Submonolayers of Adsorbates on Stepped Co/Cu(100): Switching of the Easy Axis," *Phys. Rev. B* **52**, R14400-R14403 (1995).
74. S. Ould-Mahfoud, R. Mégy, N. Bardou, B. Bartenlian, P. Beauvillain, C. Chappert, J. Corno, B. Lecuyer, G. Sczigel, P. Veillet, and D. Weller, "In-Situ RHEED and Magneto-Optic Study of Ultrathin Cobalt Films on (111) Gold Substrate: Effect of a Metallic Overlayer," *Mater. Res. Soc. Symp. Proc.* **313**, 251-256 (1993).
75. B. N. Engel, M. H. Wiedmann, R. A. van Leeuwen, and C. M. Falco, "Anomalous Magnetic Anisotropy in Ultrathin Transition Metals," *Phys. Rev. B* **48**, 9894-9897 (1993).
76. D. Hartmann, W. Weber, D. A. Wesner, S. Popovic, and G. Güntherodt, "Spin-Polarized Photoemission at Interfaces of Noble Metals with Co and Fe," *J. Magn. Magn. Mater.* **121**, 160-162 (1993).
77. Ch. Würsch, C. Stamm, S. Egger, D. Pescia, W. Baltensperger, and J. S. Helman, "Quantum Oscillations in a Confined Electron Gas," *Nature* **389**, 937-939 (1997).

Received July 8, 1996; accepted for publication March 4, 1997

Rolf Allenspach IBM Research Division, Zurich Research Laboratory, CH-8803 Ruschlikon, Switzerland (ral@zurich.ibm.com). Dr. Allenspach studied physics at the Eidgenössische Technische Hochschule (ETH) in Zurich, Switzerland, and received a Ph.D. in 1986. His thesis pertained to physical aspects of spin-polarized electron spectroscopies. Then, as a Research Staff Member, he joined the IBM Zurich Research Laboratory, where he started a project on the investigation of ultrathin magnetic films. Apart from his research, he has lectured at ETH since completing his habilitation in 1994. He was elected Wohlfarth Lecturer by the Institute of Physics, London, in 1992, and received an IBM Outstanding Technical Achievement Award in 1994 for the development of a high-spatial-resolution spin-SEM and its application to the study of thin-film magnetism.

Wolfgang Weber Laboratorium für Festkörperphysik, ETH Hönggerberg, CH-8093 Zürich, Switzerland (weber@solid.phys.ethz.ch). Dr. Weber received an undergraduate degree in physics from the University of Cologne, Germany, in 1988, and a Ph.D. in physics from the Rheinisch Westfälische Technische Hochschule in Aachen, Germany, in 1992. In 1993 he joined IBM on a postdoctoral assignment to study the magnetic properties of ultrathin metallic films. Since 1996 he has been working at the Eidgenössische Technische Hochschule Zürich, Switzerland. His current research involves spin-resolved electron spectroscopies.

[[Page 024 is blank]]